

## Supporting Information

### **One-Dimensional Co-crystallized Coordination Polymers Showing Reversible Mechanochromic Luminescence: Cation-Anion Interaction Directed Rapid Self-Recovery**

Yongsheng Yang,<sup>ab</sup> Xiaoyu Fang,<sup>a</sup> Si-Si Zhao,<sup>b</sup> Fengyang Bai,<sup>b</sup> Zhen Zhao,<sup>b</sup> Ke-Zhi Wang,<sup>\*,a</sup>  
Dongpeng Yan<sup>\*,ac</sup>

---

<sup>a</sup> Beijing Key Laboratory of Energy Conversion and Storage Materials, College of Chemistry,  
Beijing Normal University, Beijing 100875, P. R. China.

E-mail: yandp@bnu.edu.cn; kzwang@bnu.edu.cn

<sup>b</sup> Institute of Catalysis for Energy and Environment, College of Chemistry and Chemical  
Engineering, Shenyang Normal University, Shenyang 110034, P. R. China.

<sup>c</sup> College of Chemistry and Molecular Engineering, Zhengzhou University, Zhengzhou  
450001, P. R. China.

## EXPERIMENTAL SECTION

**Materials:** Analytically pure  $\text{Cd}(\text{NO}_3)_2 \cdot 4\text{H}_2\text{O}$ , anthracene-9-carboxylic acid (9HAC) and benzimidazole (BIM) were purchased from the Sigma Chemical. Co. Ltd. and used without further purification.

**Characterization:** Single-crystal X-ray diffraction data were collected at room temperature (293 K) on an Oxford Diffraction SuperNova area-detector diffractometer using mirror optics monochromated Mo  $K\alpha$  radiation ( $\lambda = 0.71073 \text{ \AA}$ ). CrysAlisPro<sup>1</sup> was used for data collection, data reduction and empirical absorption correction. The crystal structure was solved by direct methods, using SHELXS-2014 and least-squares refined with SHELXL-2014<sup>2</sup> using anisotropic thermal displacement parameters for all non-hydrogen atoms. The crystallographic data for 1D-Cd-9AC and 1D-Cd-9AC-HBIM are listed in Table S1. Crystallographic data for the complex structure in this work have also been deposited with the Cambridge Crystallographic Data Centre (CCDC) as deposition nos. CCDC 1949835 and 1950177 (available free of charge, on application to the CCDC, 12 Union Rd., Cambridge CB2 1EZ, U.K.; e-mail [deposit@ccdc.cam.ac.uk](mailto:deposit@ccdc.cam.ac.uk)). Powder X-ray diffraction analyses (PXRD) patterns were collected on a Rigaku Ultima-IV automated diffraction system with Cu  $K\alpha$  radiation ( $\lambda = 1.5406 \text{ \AA}$ ). Measurements were made in a  $2\theta$  range of  $5\text{--}50^\circ$  at room temperature with a step of  $0.02^\circ$  ( $2\theta$ ) and a counting time of 0.2 s/step. The operating power was 40 kV and 50 mA. Room temperature time-resolved photoluminescence (PL) experiments were conducted on an Edinburgh FLS980 fluorescence spectrometer equipped with a xenon arc lamp (Xe900) and a microsecond flash-lamp (uF900), respectively. The PL lifetimes ( $\tau$ ) of solid-state samples were obtained by fitting the decay curve with a multi-exponential decay function of  $I(t) = A_1 \exp(-t/\tau_1) + A_2 \exp(-t/\tau_2) + \dots + A_i \exp(-t/\tau_i)$ , where  $A_i$  and  $\tau_i$  represent the amplitudes and lifetimes of the individual components for multi-exponential decay profiles. Bright-field optical images and fluorescence microscopy images were taken from an inverted fluorescence microscope (Nikon Ti-U), by exciting the samples with a mercury lamp. IR spectra were recorded in the range of

4000–400  $\text{cm}^{-1}$  on a Tensor 27 OPUS (Bruker) FT-IR spectrometer. Thermogravimetric analysis (TGA) experiments were carried out on a Perkin-Elmer Diamond SII thermal analyzer from room temperature to 700 °C with a heating rate of 10 °C  $\text{min}^{-1}$ . Elemental analyses (C, H, O, and N) were performed on a Vario EL elemental analyzer. Solid-state UV-vis spectra were measured on a UH4150 HITACHI Spectrophotometer. The PL quantum yield (PLQY) values at room temperature were estimated using a Teflon-lined integrating sphere (F-M101, Edinburgh, diameter 150 mm and weight 2 kg) in an FLS980 fluorescence spectrometer.

**Electronic structure calculations:** The molecular structures were optimized and characterized as energy minima by the Becke three-parameter exchange functional with the Lee-Yang-Parr correction functional (B3LYP<sup>3-4</sup>) in the Gauss 09 package.<sup>5</sup> We have adopted the 6-31G(d) basis set for C, H, O and N atoms, while the LANL2DZ basis set is used for the Cd atom in connection with effective core potential (ECP) because ECP reduces the required basis set size and, more importantly, accounts for the scalar relativistic effect. The calculation of the infrared absorption frequencies is carried out at the same level.

Total/partial electronic density of states (TDOS/PDOS) analyses were performed with the periodic density functional theory (DFT) method using the Dmol3<sup>6-7</sup> module in the Material Studio software package.<sup>8</sup> The initial configuration was fully optimized by the Perdew-Wang (PW91)<sup>9</sup> generalized gradient approximation method with the double numerical basis sets plus polarization function (DNP). The core electrons for metals were treated by effective core potentials. The self-consistent field converged criterion was within  $1.0 \times 10^{-5}$  hartree  $\text{atom}^{-1}$ , and the converging criterion of the structure optimization was  $1.0 \times 10^{-3}$  hartree bohr<sup>-1</sup>. The Brillouin zone is sampled by  $1 \times 1 \times 1$  k-points, and test calculations reveal that the increase of *k*-points does not affect the results.

**Synthesis of 1D-9HAC (9HAC):** 9HAC (0.4 mmol, 0.088 g) was dissolved in a mixed solution of CH<sub>3</sub>CN (5 mL) and water (5 mL), and stirred for 3 hours at ambient temperature to get a clear solution. The final solution was filtered, and the filtrate was

allowed to evaporate at room temperature. After a few days, the light yellow rod crystals were obtained. Yield: 70%. Anal. Calcd (Found) for  $C_{15}H_{10}O_2$ : C, 81.08 (80.21); H, 4.50 (4.58); O, 14.41 (15.21).

**Synthesis of 1D-Cd-9AC ( $[Cd(9AC)_2(H_2O)_2]$ ):** A mixture of  $Cd(NO_3)_2 \cdot 4H_2O$  (0.4 mmol, 0.128 g), 9HAC (0.4 mmol, 0.088 g),  $CH_3CN$  (2 mL) and water (8 mL) was sealed in a 23 mL Teflon reactor kept under autogenous pressure at 150 °C for 72 hours and then cooled at a speed of 10 °C per minute to room temperature. Light yellow rod crystals were filtered off, washed with distilled water and ethanol in turn, and dried in air. Yield: 65% (based on Cd). Anal. Calcd (Found) for  $C_{30}H_{22}CdO_6$ : C, 60.92 (59.85); H, 3.72 (3.94); O, 16.25 (17.02).

**Synthesis of 1D-Cd-9AC-HBIM ( $[Cd(9AC)_4] \cdot (HBIM)_2$ ):** A mixture of 9HAC (0.4 mmol, 0.088 g) and BIM (0.2 mmol, 0.026 g) was added to an aqueous solution (10 mL). After stirring for 3 hours at 50 °C, a  $CH_3CN$  solution (10 mL) of  $Cd(NO_3)_2 \cdot 4H_2O$  (0.4 mmol, 0.128 g) was added to this mixture. Stirring of the resultant mixture was continued for three hours at 50 °C. The final solution was filtered, and the filtrate was allowed to evaporate at room temperature. After few days, the yellow rod crystals were obtained. Yield: 55% (based on Cd). Anal. Calcd (Found) for  $C_{74}H_{50}CdN_4O_8$ : C, 71.87 (70.08); H, 4.05 (4.25); O, 10.36 (11.44); N, 4.53 (4.12).

#### **Crystal Structures of 1D-9HAC, 1D-Cd-9AC and 1D-Cd-9AC-HBIM:**

Three one-dimensional (1D) chain polymers (1D-9HAC, 1D-Cd-9AC, 1D-Cd-9AC-HBIM) were synthesized by solvent evaporation and hydrothermal method. The 1D-9HAC crystallizes in the monoclinic  $P2_1/n$  space group (No. 14), in which 9HAC molecule form dimers by  $O-H \cdots O$  (1.824 Å, 174.5°) hydrogen bonding between the adjacent carboxyl groups and extend into a 1D chain by  $C-H \cdots O$  (2.714 Å, 147.6° and 2.777 Å, 134.6°) hydrogen bonds along the *b*-axis. The adjacent 1D chains are stabilized by an interlayer  $\pi \cdots \pi$  interaction between the aromatic rings of 9HAC ligands. The single-crystal X-ray analysis of 1D-Cd-9AC polymer reveals that its crystal structure belongs to the orthorhombic system with space group  $Pnca$  (No. 60). The 1D chain is formed by the alternating connection of  $Cd^{2+}$  metal and  $9AC^-$  ligand through coordination bonds along the *a*-axis. Each node  $CdO_8$  polyhedron is formed

by four 9AC<sup>-</sup> ligands and two coordinated water molecules. Two of the four 9AC<sup>-</sup> ligands coordinated with the Cd<sup>2+</sup> metal monodentate, and two are bidentate ligands. In addition, each 9AC<sup>-</sup> ligand forms an O–H···O (1.939 Å, 136.9°) hydrogen bond with the coordinating water molecule. The four 9AC<sup>-</sup> ligands are coordinated to the metal, and expand in four different directions. There is a large amount of C–H···π interaction between 9AC<sup>-</sup> ligands of the adjacent 1D-Cd-9AC 1D chains to stabilize the structure.

1D-Cd-9AC-HBIM, as a cocrystallized anion-cation-organized CP, belongs to the monoclinic system with a space group of C2/c (No. 15). Each building unit consists of one Cd<sup>2+</sup> cation, four 9AC<sup>-</sup> anions, and two HBIM<sup>+</sup> cation. The negatively charged CdO<sub>8</sub> polyhedron is formed by eight oxygens from four bidentate carboxylate groups of four 9AC<sup>-</sup> chelating ligands. The anionic polyhedrons are connected by N–H···O (1.778 Å, 177.5° and 1.825 Å, 155.5°) hydrogen bonds between protonated HBIM<sup>+</sup> and deprotonated 9AC<sup>-</sup> to form a 1D chain along the *c*-axis. Similarly to 1D-Cd-9AC polymer, there is no interaction between the coordinated 9AC<sup>-</sup> ligands, while there are some C–H···π interactions between the adjacent 1D chains in Cd-9AC-HBIM.

#### **Thermal Stability of 1D-9HAC, 1D-Cd-9AC and 1D-Cd-9AC-HBIM:**

Differential scanning calorimetry (DSC) and thermogravimetric analysis (TGA) were employed to investigate the thermal stability of these three polymers (**Fig. S2**). It can be observed that weight loss occurs below 200 °C in all three CPs. This part of the weight loss can be attributed to the solvent molecules in the structure. The difference is that the weight loss curve of 1D-9HAC and 1D-Cd-9AC-HBIM is smooth, and there is no obvious peak under 200 °C in the DSC curve, indicating that these solvent molecules, which were introduced during preparation, belong to the free acetonitrile or water molecule and are outside the lattice. However, for 1D-Cd-9AC, obvious steep slopes appeared in the TG curve, while inverted peaks appeared in the DSC curve under 200 °C. In DSC curves, three endothermic or exothermic peaks can be clearly observed. For 1D-9HAC and 1D-Cd-9AC-HBIM, the temperature (220 and 228 °C) corresponding to the inverted endothermic peak represents the collapse

temperature of the structure. For 1D-Cd-9AC, the exothermic peak at 353 °C indicates that at this temperature the crystalline structure changes and subsequently disintegrates. The structural changes during exotherm may be due to the rare eight-coordinate rigid chain configuration. It can indicate that the material has undergone structural changes above this temperature. Therefore, the thermal stability temperatures of these three structures are 220, 353, and 228 °C, respectively.

In TGA curves, for 1D-9HAC, the initial weight loss in the range from room temperature to 180 °C accompanying the weight loss of 4.8% is due to the removal of the free acetonitrile molecule. As the temperature rises to 700 °C, the weight loss reach to ca. 100%, indicating the structure collapses totally. For 1D-Cd-9AC, the initial weight loss in the range from room temperature to 150 °C accompanying the weight loss of 6.7% (calculated theoretical value: 6.1%) is due to the removal of the coordinating water molecule. The 9AC<sup>-</sup> ligands in the structure gradually collapsed from 353 to 700 °C. The remaining weight for 1D-Cd-9AC is 21.8%, which can be assigned to residual cadmium oxide (calculated theoretical values: 21.7%). For 1D-Cd-9AC-HBIM, the initial weight loss in the range from room temperature to 180 °C accompanying the weight loss of 2.5% is due to the removal of the free acetonitrile or water molecule. The weight loss of ~87.4% occurs in the temperature range from 228 to 700 °C, which is related to the decomposition of 9AC<sup>-</sup> and HBIM<sup>+</sup> ligands. The remaining weight is 10.1%, which can be assigned to cadmium oxide (calculated theoretical values: 10.2%). The thermal stability of 1D-Cd-9AC is better than that of 1D-9HAC and 1D-Cd-9AC-HBIM. This is because the connection between the 1D chain structural units organized by both the weak hydrogen bonds and strong coordination bonds, which constitutes a 1D rigid skeleton and thus enhances stability.

## REFERENCES

- [1] CrysAlisPro, *Rigaku Oxford Diffraction*, Version 1.171.39.6a, Rigaku Corp., Oxford, UK **2015**.
- [2] G. M. Sheldrick, *Acta Crystallogr., Sect. A*, 2008, **64**, 112–122.
- [3] A. D. Becke, *Phys. Rev. A*, 1988, **38**, 3098–3100.
- [4] A. D. Becke, *J. Chem. Phys.*, 1993, **98**, 5648–5652.
- [5] F. Bai, S. Ni, Y. Tang, X. Pan and Z. Zhao, *Phys.Chem.Chem.Phys.*, 2019, **21**, 17378–17392.
- [6] B. Delley, *J. Chem. Phys.*, 1990, **92**, 508–517.
- [7] B. Delley, *J. Chem. Phys.*, 2000, **113**, 7756–7764.
- [8] Dmol3 Module. MS Modeling, version 2.2; Accelrys Inc.: SanDiego, CA, 2003.
- [9] J. P. Perdew, J. A. Chevary, S. H. Vosko, K. A. Jackson, M. R. Pederson, D. J. Singh and C. Fiolhais, *Phys. Rev. B: Condens. Matter Mater. Phys.*, 1992, **46**, 6671–6687.

**Table S1.** Crystal data and structure refinements for 1D-9HAC, 1D-Cd-9AC and 1D-Cd-9AC-HBIM

Complex	1D-9HAC	1D-Cd-9AC	1D-Cd-9AC-HBIM
Formula	C <sub>15</sub> H <sub>10</sub> O <sub>2</sub>	C <sub>30</sub> H <sub>22</sub> CdO <sub>6</sub>	C <sub>74</sub> H <sub>50</sub> CdN <sub>4</sub> O <sub>8</sub>
<i>Mr</i>	222.24	590.87	1235.58
Temperature (K)	296	293(2)	293(2)
Crystal system	monoclinic	orthorhombic	monoclinic
Space group	<i>P2<sub>1</sub>/n</i>	<i>Pnca</i>	<i>C2/c</i>
Crystal size (mm)	0.46 × 0.31 × 0.16	0.33 × 0.12 × 0.12	0.28 × 0.28 × 0.23
<i>a</i> (Å)	3.897(3)	7.5033(3)	24.4932(11)
<i>b</i> (Å)	9.355(2)	16.7674(7)	13.5836(5)
<i>c</i> (Å)	28.980(3)	19.8262(9)	18.0604(8)
$\alpha$ (°)	90	90	90
$\beta$ (°)	90.79(4)	90	97.554(4)
$\gamma$ (°)	90	90	90
<i>V</i> (Å <sup>3</sup> )	1056.4(8)	2494.35(18)	5952.3(4)
<i>Z</i>	4	4	4
<i>D</i> <sub>calc</sub> (mg/m <sup>3</sup> )	1.397	1.573	1.379
$\theta$ Range (°)	2.0-27.5	3.147-26.371	3.26-26.37
F (000)	464	1192	2536
Data/restraint/parameters	1638 / 0 / 159	2552 / 304 / 316	6079 / 0 / 393
Reflections collected	2934	5691	11382
Independent reflections	2562	2552	6079
Goodness-of-fit on F <sup>2</sup>	1.60	1.196	0.850
<i>R</i> <sub>int</sub>	0.017	0.0523	0.0311
<i>R</i> <sub>1</sub> [ <i>I</i> >2 $\sigma$ ( <i>I</i> )]	0.044	0.0856	0.0406
<i>wR</i> <sub>2</sub> [ <i>I</i> >2 $\sigma$ ( <i>I</i> )]	0.049	0.0980	0.1149
<i>R</i> <sub>1</sub> (all data)	-	0.1605	0.0547
<i>wR</i> <sub>2</sub> (all data)	-	0.1898	0.1383

$$R_1 = \Sigma(|F_o| - |F_c|)/|F_o|; wR_2 = \{\Sigma[(w|F_o|^2 - |F_c|^2)^2/\Sigma_w(F_o)_2]\}^{1/2}$$

**Table S2.** Photophysical Properties of 1D-B and 1D-G Measured at Room Temperature ( $\lambda_{\text{ex}} = 349 \text{ nm}$ )

1D-Cd-9AC-HBIM	$\lambda_{\text{em}}$ (nm)	$\Phi_{\text{PL}}$ (%)	$\tau$ ( $\mu\text{s}$ )
1D-B	479	1.54	7.10
1D-G	498	2.79	8.60

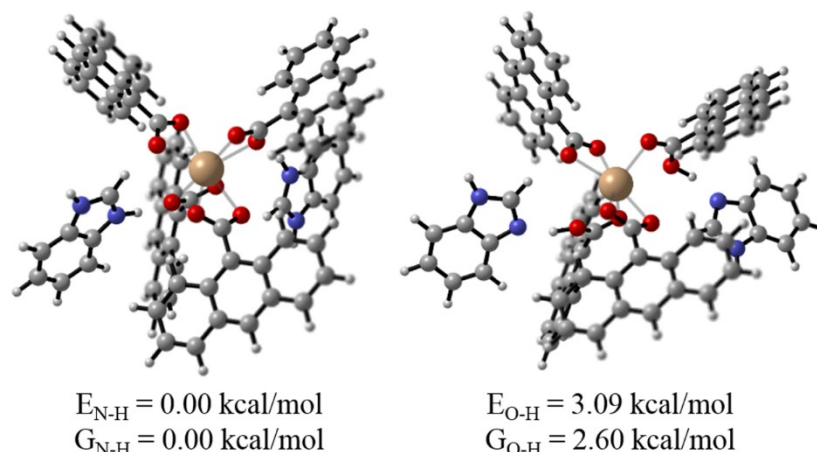


**Fig. S1.** Theoretical calculation of relative energy (E) and Gibbs free energy (G) in Cd-9AC-HBIM and Cd-9HAC-BIM structures.

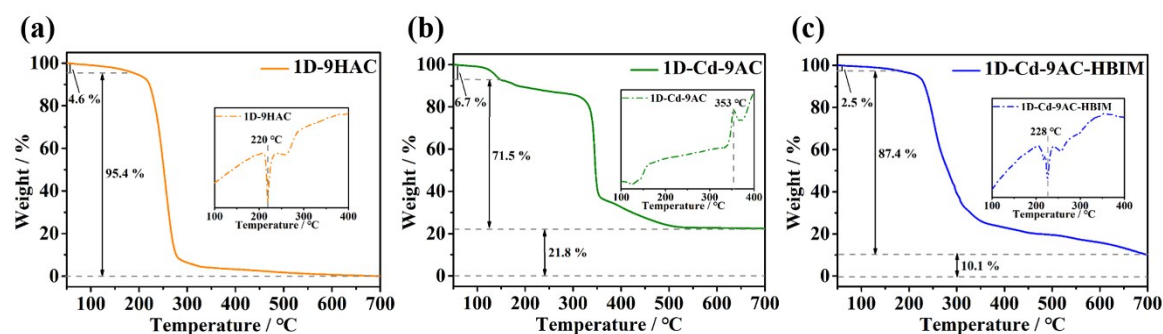


**Fig. S2.** Differential scanning calorimetry (DSC) and thermogravimetric analysis (TGA) curves of 1D-9HAC (a), 1D-Cd-9AC (b) and 1D-Cd-9AC-HBIM (c).

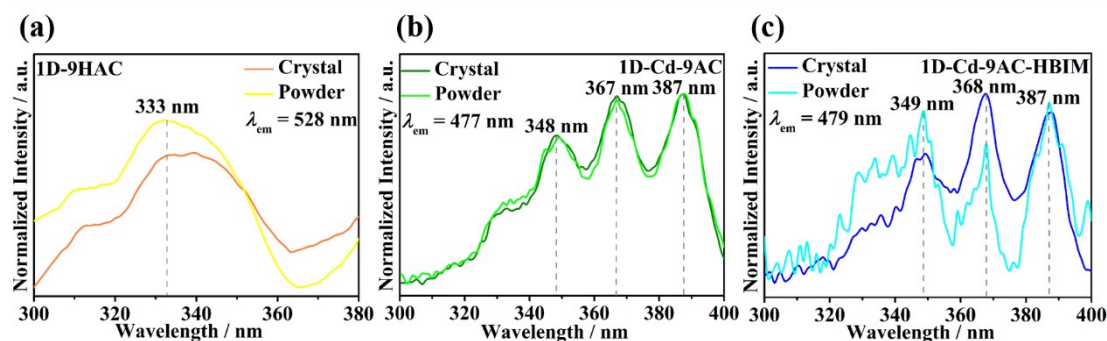


**Fig. S3.** Normalized fluorescence excitation spectra of 1D-9HAC (a) ( $\lambda_{\text{em}} = 528 \text{ nm}$ ), 1D-Cd-9AC (b) ( $\lambda_{\text{em}} = 477 \text{ nm}$ ) and 1D-Cd-9AC-HBIM (c) ( $\lambda_{\text{em}} = 479 \text{ nm}$ ) in their powder and crystal states.

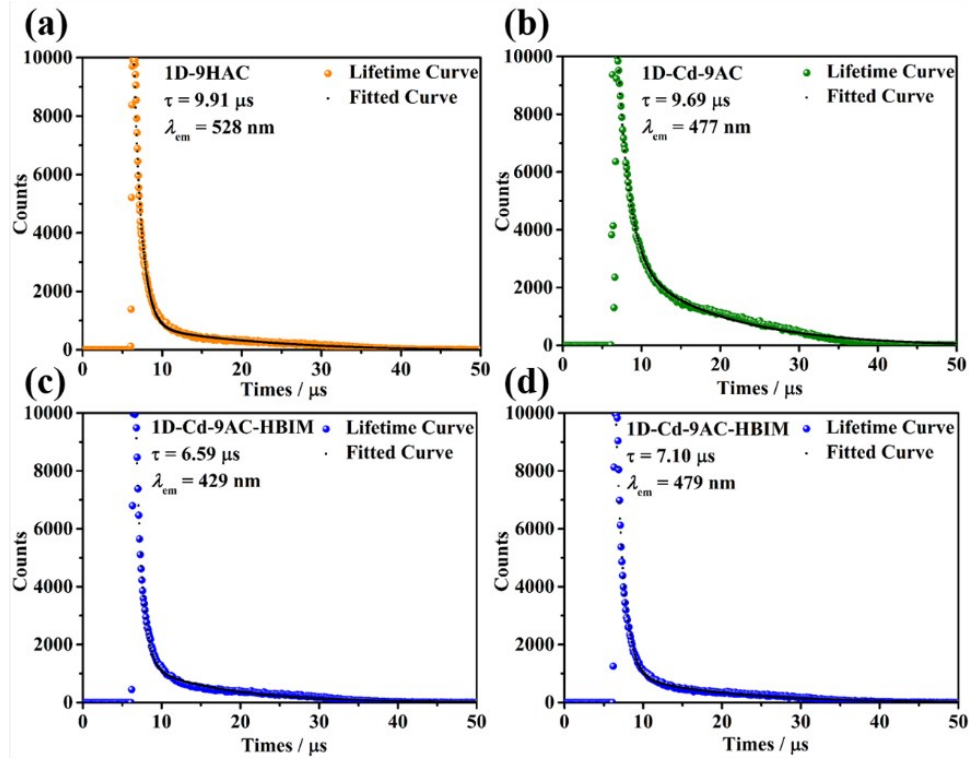


**Fig. S4.** Time-resolved emission decay curves for 1D-9HAC ( $\lambda_{em} = 528$  nm) (a), 1D-Cd-9AC ( $\lambda_{em} = 477$  nm) (b) and 1D-Cd-9AC-HBIM ( $\lambda_{em} = 429$  and 479 nm) (c, d) under ambient conditions.

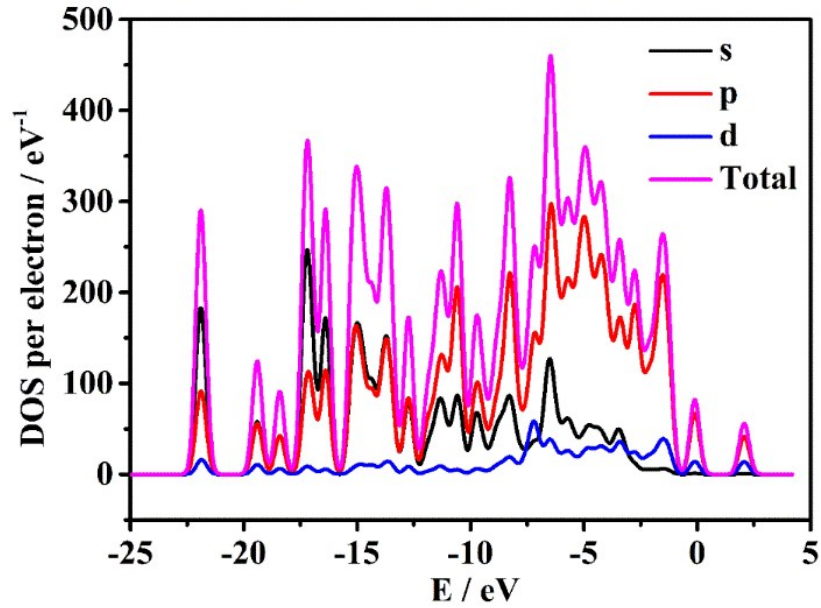


**Fig. S5.** Total/partial electronic density of states (TDOS/PDOS) for 1D-Cd-9AC-HBIM.

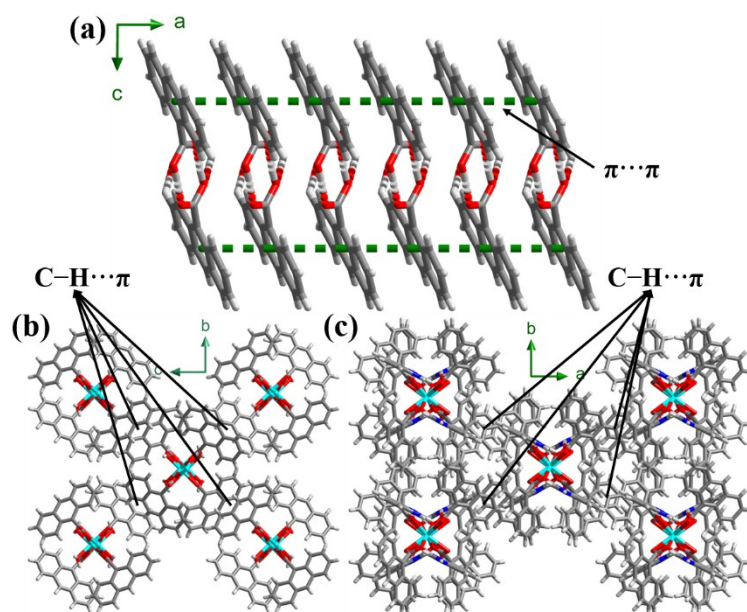


**Fig. S6.** The packing patterns of 1D chains in 1D-9HAC (a), 1D-Cd-9AC (b) and 1D-Cd-9AC-HBIM (c).

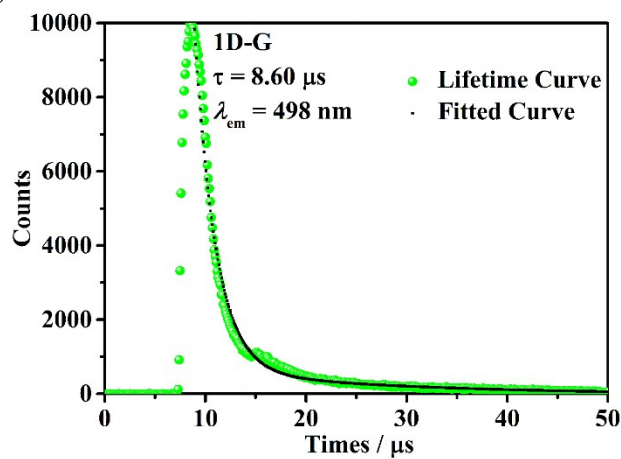


**Fig. S7.** Time-resolved emission decay curves for 1D-G ( $\lambda_{em} = 498 \text{ nm}$ ) under ambient conditions.

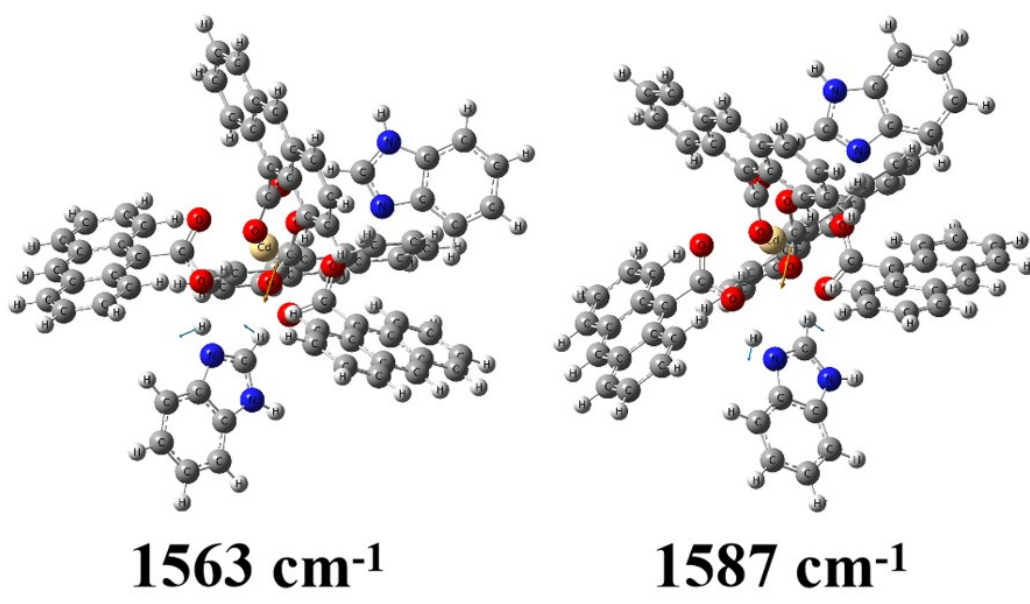


**Fig. S8.** Theoretical calculation simulation of IR spectra for 1D-Cd-9AC-HBIM.

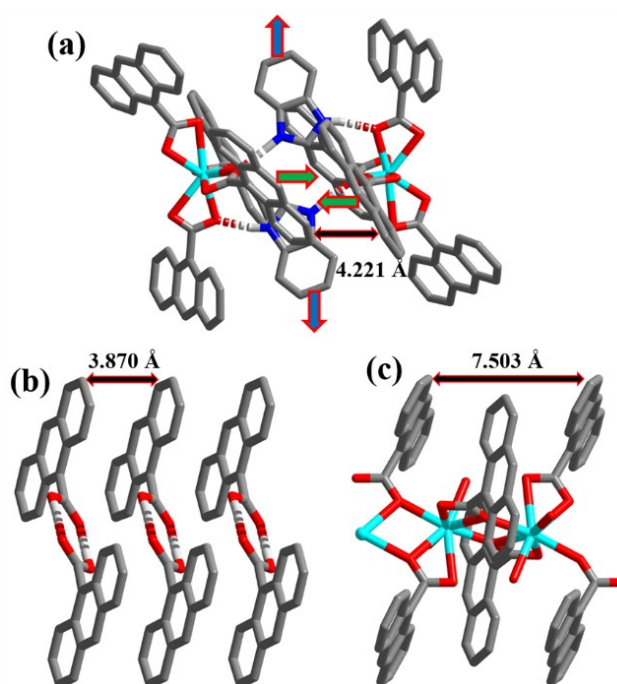


**Fig. S9.** (a) The schematic diagram of the structural change trend under grinding for 1D-Cd-9AC-HBIM. The distance of 9AC ligands in the structure for 1D-9HAC (b) and 1D-Cd-9AC (c)

For 1D-9HAC, the distance between 9HAC molecular is closely enough (3.870 Å) that it is difficult to further change the packing structure by an external force (**Fig. S9b**). For 1D-Cd-9AC, the rigid chain structure, which consists of coordination bonds and covalent bonds, also inhibits the influence of external forces on the packing mode (**Fig. S9c**).

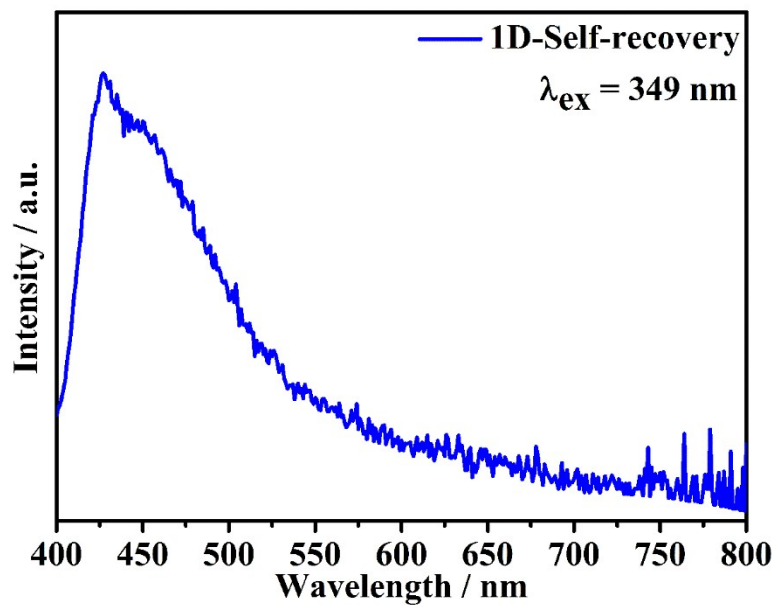


**Fig. S10.** Room-temperature solid-state photoluminescent emission spectra of 1D-Self-recovery ( $\lambda_{\text{ex}} = 349 \text{ nm}$ ).

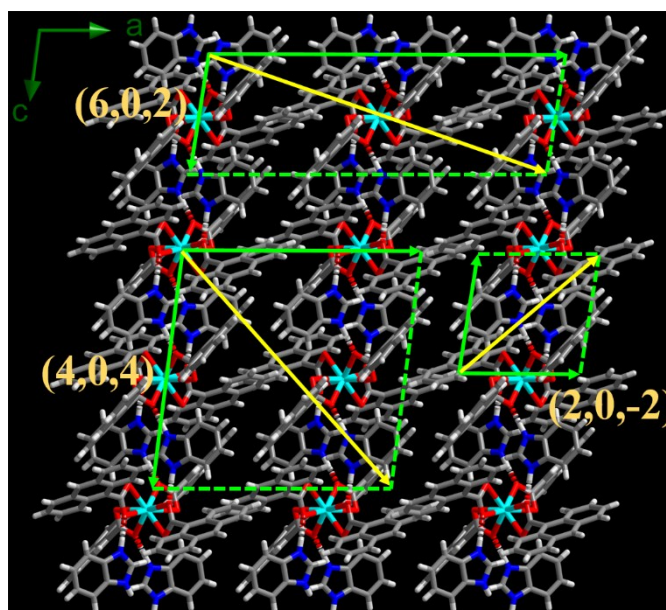


**Fig. S11.** The stacked structure of 1D-Cd-9AC-HBIM, viewed along the  $b$ -axis.

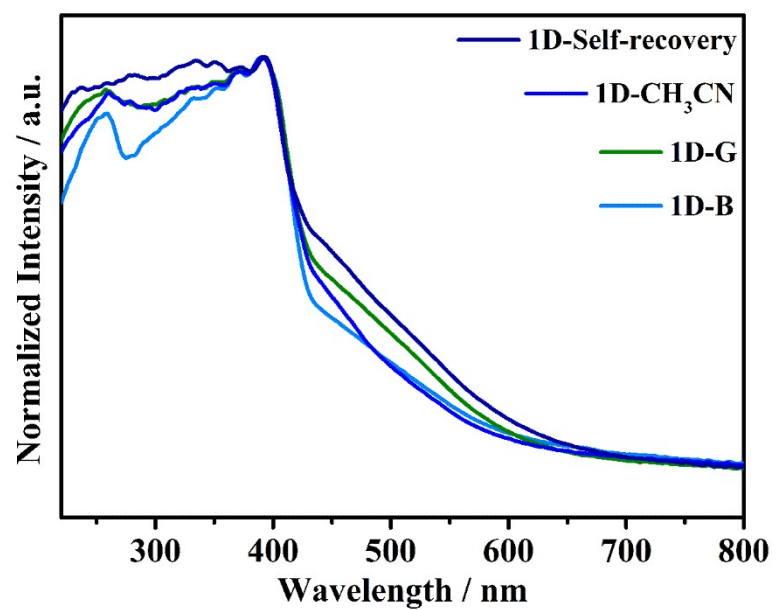


**Fig. S13.** Solid-state UV-visible absorption spectra for 1D-Cd-9AC-HBIM in different response states.